JOURNAL OF AGRICULTURAL AND FOOD CHEMISTRY
ARTICLE

J. Agric. Food Chem. 2009, 57, 10755–10764 10755
DOI:10.1021/jf901949r

Proteome Changes during Meat Aging in Tough and Tender Beef Suggest the Importance of Apoptosis and Protein Solubility for Beef Aging and Tenderization

Elisabeth Laville,*,† Thierry Sayd,† Martine Morzel,‡ Sylvie Blinet,† Christophe Chambon,§ Jacques Lepetit,† Gilles Renand,∥ and Jean François Hocquette⊥

†INRA, UR370, Qualité des Produits Animaux, Theix, 63122 Saint-Genès-Champanelle, France, ‡INRA, UMR1129 FLAVIC (Flaveur, vision et Comportement du Consommateur), 17 rue Sully, 21000 Dijon, France, §INRA, Plate-Forme d'Exploration du Métabolisme, pôle Protéome, Theix, 63122 Saint-Genès-Champanelle, France, ∥INRA, UR 337, Station de Génétique Quantitative et Appliquée, 78352 Jouy-en-Josas cedex, France, and ⊥INRA, UR1213 Unité de Recherches sur les Herbivores, Theix, 63122 Saint-Genès-Champanelle, France

Within a population of Charolais young bulls, two extreme groups of longissimus thoracis muscle samples, classified according to Warner−Bratzler shear force (WBSF) of 55 °C grilled meat, were analyzed by 2D-electrophoresis. Muscle analyses were performed on 4 bulls of the "tender" group (WBSF = 27.7 ± 4.8 N) and 4 bulls of the "tough" group (WBSF = 41.2 ± 6.1 N), at 3 post-mortem times: D0, samples taken within 10 min post-mortem; D5 and D21, samples kept at 4 °C under vacuum during 5 and 21 days. Proteins of muscle samples were separated in two fractions based on protein solubility in Tris buffer: "soluble" and "insoluble". Proteins of both fractions were separated by 2D-electrophoresis. Evolution of spots during the 3 post-mortem times was analyzed by hierarchical classification (HCA). Three clusters of proteins presenting similar evolution profiles provided accurate classification of post-mortem times and showed the translocation of some chaperone proteins and glycolytic enzymes from the soluble fraction to the insoluble fraction between D0 and D5. Cellular structure dismantlement and proteolysis was observed at D21. Effect of group ("tender" vs "tough") on spot intensities was tested by ANOVA. At D0, higher quantity of proteins of the inner and outer membrane of mitochondria was found in the tender group suggesting a more extensive degradation of mitochondria that may be related to the apoptotic process.

KEYWORDS: Proteome analysis; beef muscle; tenderness; hierarchical clustering analysis; protein solubility; proteolysis; HSP27; glycolytic enzymes; mitochondrial membrane

INTRODUCTION

Tenderness is one of the most important attributes influencing consumption of beef meat (*1*), but there is a large variation in the rate and extent of post-mortem tenderization, and this is one of the causes of inconsistency in meat tenderness at the consumer level.

The major eating qualities of meat are developed during muscle aging, and it is well established that storage improves meat tenderness. A number of studies unanimously recognized that the meat tenderizing process results from proteolysis of myofibrillar and associated structural proteins. These proteins ensure inter- and intramyofibril linkage and attach myofibrils to sarcolemma by costameres. Proteolysis of these proteins causes weakening of the structures and thus tenderization. Proteolysis involves different proteolytic systems and their inhibitors: calpain, calpastatin, cathepsin, proteasome and more recently described caspase and serpin (for a review see refs *2* and *3*).

*Corresponding author. Tel: +33 (0)4 73 62 48 34. Fax: +33 (0)4 73 62 42 68. E-mail: elaville@clermont.inra.fr.

During post-mortem aging, muscle proteins are also subjected to denaturation, which is related to intracellular pH decline resulting from post-mortem anaerobic glycolysis. The process is commonly described in species such as pig and poultry, having more glycolytic muscle fiber types (*4*). Different studies on pig meat suggest that protein denaturation during post-mortem aging may influence proteolysis. These studies report a lower degree of myofibrillar protein degradation during post-mortem aging in pale, soft, exudative (PSE) pig meat (*5*−*8*) which was partly explained by the earlier inactivation of endogenous proteolytic action, due to increased early post-mortem muscle temperature (*9*−*12*), and/or lower early post-mortem pH (*13*). It was further suggested that accessibility of myofibrils to endogenous proteolytic action may be reduced in PSE pig meat (*14*) due to increased protein aggregation and coprecipitation of glycolytic enzyme fragments onto myofibrils (*15*). Because muscles of bovines are less glycolytic, post-mortem anaerobic glycogenolysis and acidification rate are less pronounced. However, post-mortem protein insolubilization processes according to pH level

Published on Web 10/27/2009

are described. Pulford (*16*) demonstrate that the disappearance of chaperone proteins (HSP27 and α-crystallin) from the soluble phase of beef muscle extracts was due to increasing muscle acidity in post-mortem stages. The level of HSPs was found dynamic over the first 22 h period post-mortem, and these authors suggested that the effect of the ultimate pH upon the solubility of HSPs may influence meat tenderization. Other authors have also demonstrated a relationship between the gene expression of another HSP (DNAJA1) and beef toughness (*17*) (Bernard et al., 2007).

Conversion of muscle to meat implies complex and interdependent biochemical mechanisms, and the influence of these mechanisms on the final texture and tenderness of the meat is still not clear. With the objective to refine knowledge of molecular mechanisms involved in the development of meat tenderness, using two-dimensional electrophoresis (2-DE), the current study was designed to follow post-mortem proteome modifications in two groups of beef longissimus muscles selected for shear force of cooked meat. We compared the proteomic profiles at three post-mortem times (10 min after bleeding and after 5 and 21 days of aging). In order to increase gel resolution (the number of proteins that can be detected and quantified) we separated the muscle extracts in two fractions according to protein solubility and performed gel electrophoresis on each fraction.

MATERIALS AND METHODS

Animals and Carcass Sampling. The animals used in the experiment were 64 young Charolais bulls weaned at 32 weeks and then reared in an open shed. They were fed a complete pelleted diet distributed ad libitum with a limited amount of straw until slaughter. Half of randomly chosen animals were slaughtered at 15 months of age and half at 19 months of age to take account of variability of physiological traits according to growing stages. Bulls were slaughtered in the same experimental abattoir as previously described (*17*). Longissimus thoracis (LT) muscles were sampled at the sixth rib position. A first sample (1 g) was excised with a corer immediately after skinning, snap frozen in liquid nitrogen and subsequently stored at −80 °C for proteomic analysis. Such sample corresponded to D0 (within 10 min post-mortem). Carcasses were chilled at 12 °C from 1 h post-mortem during 4 h and then stored at 3 °C. Twenty-four hours post-mortem, about 5 g of muscle was sampled. The excised sample was cut in two pieces, which were individually vacuum-packed and stored at 4 °C until 5 days (D5) and 21 days (D21) of aging when pieces were snap frozen in liquid nitrogen and subsequently stored at −80 °C for further proteomic analysis. Meat ultimate pH (pH_u) was recorded on the longissimus muscle on the level of the last rib 24 h post-mortem using an Ingold Xerolyt penetration gel electrode (Mettler Toledo SA, Viroflay, France) and a portable Knick 911 pH meter (Knick Elektronische Messgeräte GmbH & Co., Berlin, Germany). The shear force was determined on aged and cooked meat corresponding to a status in which meat is consumed. LT steaks including the ninth rib were vacuum packaged at 24 h post-mortem, aged at 4 °C for 21 days and stored at −20 °C. After thawing during 1 h in running water, steaks were cut to a thickness of 3 cm. They were then grilled simultaneously on both sides (model Infragrill E, Sofraca, France) until a core temperature of 55 °C was reached.

Shear Force Measurements on Cooked Meat. Rectangular meat samples (section = 1 cm^2) were sheared perpendicularly to muscles fibers with a Warner−Bratzler cell fitted on an universal testing machine (Instron France S.A.S., Guyancourt, France). The cell and the test follow the recommendations of Honikel (*18*). All shear force measurements were performed with prior cooling of meat at room temperature. The mean values are obtained from 10 to 12 measurements.

Protein Extraction. Proteomic analysis was carried out on the LT samples referred to above as D0, D5 and D21. Protein extraction was carried out on 1 g of muscle as previously described (*19*). Briefly, muscle was homogenized, using a glass bead agitator MM2 (Retsch, Haan, Germany), in 40 mM Tris (pH 8), 2 mM EDTA and a protease inhibitors cocktail (SIGMA) at 4 °C, at the ratio of 1:4 (w/v). The homogenate was centrifuged at 4 °C for 10 min at 10000*g*. The supernatant, referred to as the "soluble" in the Tris buffer fraction, was stored at −80 °C until further assaying. The pellet was washed four times by homogenization in the above buffer using the glass bead agitator MM2 and centrifugation at 4 °C for 10 min at 10000*g*. Finally, the pellet was resuspended, solubilized using a glass bead agitator MM2 (Retsch, Haan, Germany) for one hour at 4 °C, in the extraction buffer consisting of 7 mM urea, 2 M thiourea, 4% (w/v) CHAPS, 1% (w/v) DTT and protease inhibitors cocktail (SIGMA). Extracts were centrifuged at 10000*g* for one hour at 10 °C. The supernatant, referred to as the "insoluble" in the Tris buffer fraction, was collected and stored at −80 °C until further assaying. The last pellet was discarded. Protein concentration was determined by the Bradford assay (BioRad, Hercules, CA).

Two Dimensional Gel Electrophoresis. 900 μg of protein extracts was included in a buffer containing 7 M urea, 2 M thiourea, 2% (w/v) CHAPS 0.4% (v/v) carrier ampholyte and bromophenol blue. Samples were loaded onto immobilized pH-gradient strips of 17 cm (BioRad). The chosen pH-gradients of strips were 5−8 and 3−10 NL, respectively, for soluble and insoluble fractions. The isoelectric focusing was performed using a Protean IEF cell system (BioRad). Gels were passively rehydrated for 16 h. Rapid voltage ramping was subsequently applied to reach a total of 85 kV h. In the second dimension, proteins were resolved on 12% SDS−PAGE gels using Protean II XL system (BioRad). Gels were Coomassie Blue (colloidal blue) stained as previously described (*20*). Three gels were produced per sample. Technical variability was assessed (variation coefficient of 24.3%) and found lower than biological variability.

Gel Visualization, Image Acquisition, and Statistical Analysis. Gel images were acquired using a GS-800 imaging densitometer (BioRad) and analyzed using the two-dimension electrophoresis (2DE) image analysis software PDQuest (BioRad). Image analysis was performed as previously described (*19*). The intensity-dependent distribution of spots was assessed according to the technique of Meunier (*21*) and found to be normal. A hierarchical clustering analysis (HCA) using the PermutMatrix software (http://www.lirmm.fr/~caraux/PermutMatrix/; LIRMM, Montpellier, France) was performed after a log-ratio transformation of averaged detected and matched spot intensities. Data of soluble and insoluble fractions were merged in the same table. The objective was to explore and visualize which spots have similar expression profiles during aging (*22*). The Ward dissimilarity aggregation procedure based on Pearson distances was used as recommended by Meunier (*23*). The one way HCA was applied to the row (spot intensities) in order to construct a dendrogram of proteins presenting similar evolution profiles according to post-mortem time. In addition, the ANOVA procedure was used to test significance ($p < 0.05$) of the fixed effect of group (tender vs tough) at each post-mortem time on log-ratio values of averaged intensities of detected and matched spots. Statistical analyses were performed using SAS software version 8 (SAS Inst., Inc.; Cary, NC). One-sided binomial analysis was used to assess whether the proportion of spots influenced by group was greater than the proportion expected by chance (5%). Where significant effects were found, Bonferroni comparison tests were used to identify differences between groups at the 5% significance level.

In-Gel Digestion and Proteins Identification by Mass Spectrometry. Coomassie stained spots of interest were manually excised using pipet tips. The spots were then destained with 100 μL of 25 mM NH_4HCO_3 and 5% v/v acetonitrile for 30 min, followed by 100 μL of 25 mM NH_4HCO_3 and 50% v/v acetonitrile and then dehydrated in acetonitrile. Gel spots were completely dried using a Speed Vac before trypsin digestion at 37 °C over 5 h with 15 μL of trypsin (10 ng/μL; V5111, Promega, Madison, WI) in 25 mM NH_4HCO_3. Peptide extraction was optimized by adding 8 μL of acetronitile, followed by 5 min of sonication. For matrix-assisted laser desorption/ionization−time-of-flight (MALDI-TOF) mass spectrometry analysis, 1 μL of supernatant was loaded directly onto the MALDI target. The matrix solution (5 mg/mL of α-cyano-4-hydroxy-cinnamic acid in 50% acetonitrile, 0.1% trifluoroacetic acid) was immediately added and allowed to dry at room temperature.

Peptide mass fingerprint (PMF) of trypsin digested spots was determined in positive-ion reflector mode using a Voyager DE Pro MALDI-TOF-MS (Applied Biosystems, Framingham, MA). External calibration was performed with a standard peptide solution (Peptide Mix 4, Proteomix, LaserBio Laboratories, Sophia-Antipolis, France). A total of

1000 shots from the nitrogen laser operating at 337 nm were accumulated for each spot. The spectra were internally calibrated using trypsin autolysis peaks followed by noise-filtration. The resulting peak lists were generated by the DataExplorer 4.0 software (Applied Biosystems). PMFs were compared to *Mammalia* SWISS Prot database (08/2008, 60811 sequences) protein sequence databases (ftp://ftp.ebi.ac.uk/pub/databases/uniprot/knowledgebase/uniprot_sprot.fasta.gz) using MASCOT 2.2 software (http://www.matrixscience.com). The initial search parameters allowed a single trypsin missed cleavage, partial carbamidomethylation of cystein, partial oxidation of methionine and mass deviation lower than 30 ppm. We required at least five matched peptides per protein for identification and used MASCOT probabilistic scores and accuracy of the experimental to theoretical p*I* and molecular weight (MW).

RESULTS AND DISCUSSION

Based on the results of the Warner−Bratzler shear force (WBSF) measurements and in order to follow the design of the experiment, two bulls in each group of age (15 and 19 months) were chosen for their low WBSF cooked value (tender, $N = 4$), and two bulls in each group of age were chosen for their high WBSF cooked value (tough, $N = 4$). Average WBSF values were 27.7 ± 4.8 N and 41.2 ± 6.1 N, in tender (Te) and tough (To) groups respectively. According to Miller (*24*) the first group corresponds to tender meat with 100% consumer satisfaction and the second group to intermediate tenderness with about 86% consumer satisfaction. The ultimate pH values of the Te and To groups were 5.51 ± 0.05 and 5.40 ± 0.19, respectively; and they were not different ($P < 0.05$). The muscle proteomic results presented below are those of these 8 bulls.

Proteomic Analysis. We matched and quantified 351 spots and 333 spots on soluble and insoluble protein 2-DE gels, respectively.

Effect of Post-Mortem Storage. We performed ANOVA analysis in order to determine which spots were modified across the three sampling times. 209 spots and 243 spots were found differential in soluble and insoluble fractions, respectively (data not shown). Most of the proteins were affected by aging. In order to synthesize information, data were treated using the HCA analysis. The objective was to determine a list of spots whose variation characterized the three aging times. Three clusters of proteins presenting similar evolution profiles according to aging were found (**Figure 1**). We identified proteins of those clusters (**Tables 1**, **2** and **3**). The "observed" MW and p*I* of spots were determined onto the gel images using the PDQuest software procedure: the MW/p*I* of spot proteins known was entered, and the pH gradient used in the first dimension was indicated. When there was an evident discrepancy between the theoretical MW of a protein and its MW estimated through its position in the gel, it was considered as "fragment".

Cluster 1 corresponded to proteins abundant at D0 and whose quantity dropped from D5. The cluster was made up of 24 spots, of which 16 were identified (**Table 1**). The cluster was mainly constituted by proteins from the soluble fraction (22/24). We identified myofibrillar proteins in this soluble fraction (one spot of actin fragment, one spot of actin, and one spot of myosin light chain 2). These proteins belong to a group of the most abundant muscle myofibrillar proteins. They are, in theory, components of the insoluble compartment, but some copies are often extracted with soluble proteins (*15*, *25*). In addition, we found regulatory proteins and chaperone proteins, part of the muscle stress response pathway, which have the property to stabilize and maintain myofibrillar structure after a challenge (heat-shock proteins, alpha β-crystallin, ankyrin, WD repeat-containing protein 1, tripartite motif-containing protein 72). Three other proteins were extracted from the soluble fraction (the mitochondrial isocitrate dehydrogenase, a biphosphoglycerate mutase and a purine synthetase). The glycolytic enzyme phosphoglucomutase extracted from the insoluble fraction had also a similar evolution profile in cluster 1.

Cluster 2 corresponded to proteins less expressed or absent at D0 and whose quantity increased at D5 and remained stable at D21. The cluster was made up of 37 spots, of which 33 were identified (**Table 2**). The cluster was mainly constituted by proteins extracted from the insoluble fraction (27/37). Interestingly, we found in the insoluble fraction at D5 (and D21) some protein species of the soluble fraction characterizing the cluster 1, namely, one spot of actin fragment having the same MW as the fragment of the D0 soluble fraction (about 30 kDa), a spot of myosin light chain 2, 6 variants of HSP27 (**Figure 2**), 2 variants of alpha β-crystallin and the WD repeat-containing protein 1. Cluster 2 contained also a spot of heat-shock protein beta-6 (another chaperone protein), and 14-3-3 protein gamma and epsilon proteins which are cytosolic proteins implicated in the regulation of a large spectrum of signaling pathways by their ability to bind to a large number of partners, including actin. In addition, the cluster was constituted by several electrophoretic isoforms of full length proteins and fragments of proteins involved in energetic metabolism namely creatine kinase (CK), the AMP deaminase activated by its binding to myosin and glyceraldehyde-3-phosphate dehydrogenase (GAPDH). Two enzymes of the mitochondrial matrix involved in citric acid cycle, namely, pyruvate dehydrogenase and dihydrolipoamide succinyltransferase, were also found in the insoluble fraction. Appearance of soluble proteins in the insoluble fraction at D5 suggests that, during the five first days of muscle aging, they had been subjected to chemical modifications that made them insoluble. Cluster 2 was also constituted by proteins of the soluble fraction. These full length proteins are involved in cell protection and signalization (HSP 27, DJ1, ubiquitin, dihydropyrimidinase-related protein 2, histidine triad nucleotide-binding protein 1 and adenylate kinase isoenzyme 1), and the phosphoglucomutase involved in glycogen metabolism. Appearance of these proteins in the soluble fraction at D5 should correspond to a release of these soluble proteins from the insoluble compartment in which they were retained at D0.

Cluster 3 corresponded to proteins absent or slightly abundant at D0 and D5 whose quantity increased at D21. The cluster was made up of 39 spots 17 proteins belonging to the soluble fraction. Only 20 spots were identified (**Table 3**). Most of the spots identified corresponded to putative fragments. Because only a few peptides can be recognized on the sequence of the parent protein recorded in databases, it is relatively difficult to identify protein fragments with classical peptide mass fingerprinting. Together with their low intensities, this explains the limited rate of successful identifications for this cluster. Some fragments were found in both fractions: HSP (27 and 70) and metabolic enzymes as for example, GAPDH, β-enolase and CK. As for CK it was interesting to observe that both spots were found at lower molecular weights than those of fragments found in cluster 2, suggesting a refragmentation. The cluster also contained two protein fragments from the soluble fraction: a first fragment of annexin A6, which binds phospholipids in a Ca(2+)-dependent manner (the protein is associated with sarcoplasmic reticulum membranes in skeletal muscle and may play a regulatory role in the Ca(2+)-release/uptake cycle); second, a fragment of vinculin, which is a component of a lateral attachment system of myofibrils to the plasma membrane. The increased abundance of fragments of these proteins and their release in the soluble fraction at D21 from cellular structures to which they are bound (membranes and myofibrillar anchoring complexes) suggests a more important degradation of these structures at 21 days post-mortem. In the

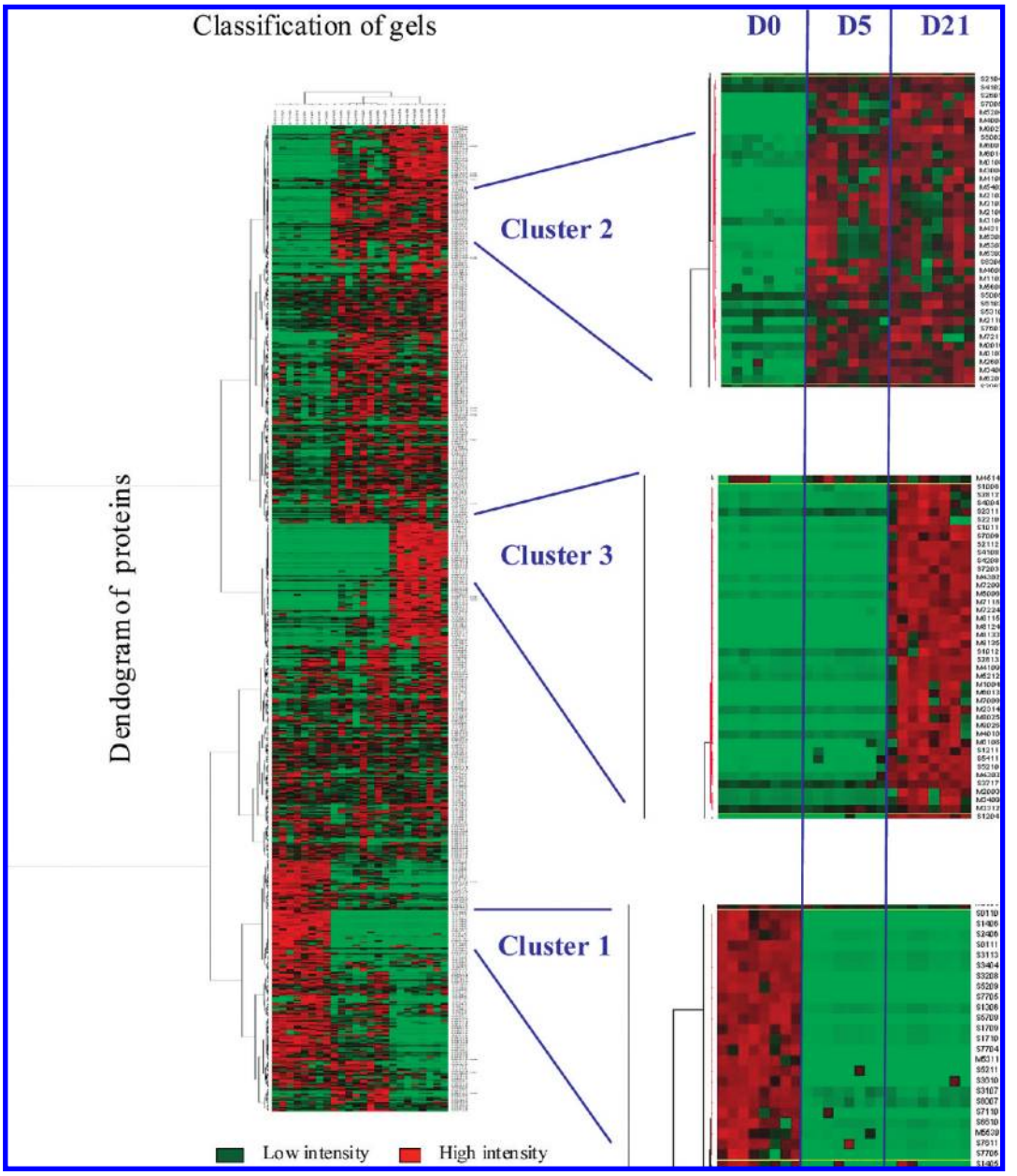

Figure 1. Heat map representation of the one-way hierarchical clustering analysis (processed with PermutMatrix according to the Pearson distance and Ward's aggregation method) after a log-ratio transformation of averaged detected and matched spot quantities. Numerical values from the data set were converted into a gradation of colors: red for a high value and green for a low value. The classification of the columns corresponding to the gels was constrained according to post-mortem time. The rows corresponding to detected and matched spot intensities of soluble and insoluble fractions were automatically permuted in such a way that a statistical organization in the data set was revealed. The dendrogram of spots allows distinguishing three clusters of proteins presenting similar evolution profiles according to post-mortem time.

same way, the presence of mitochondrial membrane VDAC-1 protein, extracted in insoluble fraction, suggests also an increase in the degradation of mitochondrial membranes. In addition, the coexpressed spot of actin may be related to the loss of structure of cellular elements.

Modifications of Protein Solubility during Aging. During post-mortem times, proteome modifications may have different causes. One modification was illustrated by the behavior of soluble proteins as for example HSP 27 and glycolytic enzymes (CK and GAPDH), which appeared in the insoluble fraction at D5. This indicates the decrease of solubility of these proteins during the first phase of aging. Decrease of protein solubility may be related to decrease of intramuscular pH during the first 24 h post-mortem due to anaerobic glycogenolysis. Boles (*5*) showed the effect of early post-mortem pH fall on the loss of solubility of some glycolytic enzymes, CK and GAPDH. They suggested that pH drop associated with high muscle temperature denatured proteins which became insoluble made aggregates and precipitated onto myofibrils. Both proteins belong to a class of redox-regulated proteins having highly reactive cysteine residues that can be modified upon exposure to oxidative stress (*26*−*28*). These modifications cause significant conformational changes and lead to either activation or inactivation of the protein function. The modification of their solubility may be related to susceptibility to oxidation. In the same way, Pulford (*16*) showed that the value of post-mortem intramuscular ultimate pH affected solubilization of the chaperone proteins HSP27, alpha β-crystallin and HSP20. Different mechanisms were proposed to explain the movement of

Table 1. Bovine Longissimus Muscle Proteins Evidenced in Cluster 1 (See **Figure** 1) According to HCA Analysis

						M_w (kDa)/p*I*		mean value		
spot no.[a]	protein ID[b]	accession no.[b]	mowse score[c]	sequence coverage[d]	MP[e]	theor[f]	obsd[f]	at D0[g]	at D5[g]	at D21[g]
S0110	myosin regulatory light chain 2	MLRV_MOUSE	85	51	11	18.7/4.71	18.9/4.86	4358	–	–
S1406	ankyrin repeat domain-containing protein 2	ANKR2_MOUSE	81	27	13	36.6/5.95	38/5.51	1036	–	–
S2406	ankyrin repeat domain-containing protein 2	Q9WV06|ANKR2_MOUSE	68	20	7	39.8/6.22	37.8/5.56	235	–	–
S0111	heat-shock protein beta-2	HSPB2_HUMAN	80	51	8	20.2/5.07	20.3/5.11	435	–	–
S3404	isocitrate dehydrogenase [NAD] subunit alpha, mitochondrial precursor	IDH3A_BOVIN	62	13	7	39.6/6.76	37.1/5.95	221	–	–
S3208	heat-shock protein beta-1 (HSP 27)	HSPB1_BOVIN	49	21	6	22.3/5.98	22.9/5.78	1615	–	–
S5209	heat-shock protein beta-1 (HSP 27)	HSPB1_BOVIN	132	62	12	22.3/5.98	22.1/6.16	5004	–	–
S3107	heat-shock protein beta-1 (HSP 27)	HSPB1_BOVIN	62	27	5	22.3/5.98	22.3/5.98	45873	1392	1043
S7705	bifunctional purine biosynthesis protein	PUR9_HUMAN	85	24	13	64.5/6.27	63.3/6.44	1258	–	–
S1306	actin, alpha cardiac muscle 1 - **Fgm**[h]	Q3ZC07|ACTC_BOVIN	72	19	6	41.9/5.23	29/5.23	128	–	–
S7704	WD repeat protein 1 (actin-interacting protein 1)	WDR1_HUMAN	141	28	18	66/6.18	67.4/6.36	1242	–	–
S7706	WD repeat protein 1 (actin-interacting protein 1)	WDR1_MOUSE	68	11	9	66.2/6.12	68.2/6.41	437	–	–
S5211	bisphosphoglycerate mutase	Q3T014|PMGE_BOVIN	100	51	12	30/6.03	25.2/6.13	649	–	–
S3610	tripartite motif-containing protein 72	Q6ZMU5|TRI72_HUMAN	64	19	7	52.6/6.05	54.8/5.86	1054	–	75
S8007	alpha-crystallin B chain -	P02510|CRYAB_BOVIN	74	37	9	20/6.76	19.6/6.84	67496	1665	2361
M5530	phosphoglucomutase-1	PGM1_MOUSE	100	27	15	61.3/6.32	63.8/6.66	130	–	–

[a] Spot number preceded by S corresponds to soluble fraction, and spot number preceded by M corresponds to insoluble fraction. [b] Protein name and accession numbers were derived from SWISS Prot database. [c] The MASCOT baseline significant score is 60. [d] % of coverage of the entire amino acid sequence. [e] Number of matched peptides in the database search. [f] MW and p*I*, theoretical (recorded in SWISS Prot database) and observed (calculated from the spot position on the gel). [g] Intensity mean value of tender and tough groups. (–) Spot intensity corresponds to intensity value lower than 15 ppm. [h] **Fgm**, protein fragment.

HSPs away from the soluble fraction. The most probable mechanism retained by Pulford (*16*) was an isoelectric precipitation. When the intracellular pH reaches the isoelectric point of a protein, the lack of a net charge reduces protein solubility and causes precipitation. Alternative mechanisms related to properties and functions of proteins of HSPs, namely, formation of oligomer complexes, interaction with unfolded proteins or interactions with myofibrils during an ischemic challenge are also possible mechanisms to explain the translocation of HSPs from cytosol to myofibrils (*29*, *30*). In addition, we identified a fragment of actin in the soluble fraction at D0 which disappeared at D5 and may be related to appearance of a fragment with a close MW in insoluble fraction at D5, suggesting that actin may be subjected to insolubilization during aging. In the same way and probably due to similar mechanisms, the spot of the myosin regulatory light chain 2 evidenced in soluble fraction at D0 disappeared from the soluble fraction and appeared in insoluble fraction at D5 and D21.

Proteolysis during Aging. The second major post-mortem modification evidenced by this experiment was proteolysis. Proteolysis could be directly observed by the increased number and intensities of spots corresponding to protein fragments. Most of them were generated between sampling times D5 and D21, and they constituted the cluster 3. Most of the fragments belonged to the most abundant glycolytic enzymes of the cytosol (CK, GAPDH, enolase, phosphoglycerate kinase) and mainly originated from the insoluble fraction, where some of these proteins have precipitated in the first step of muscle aging (between D0 and D5). Interestingly, we also found protein fragments and full length proteins belonging to cell structures like membranes or anchoring systems of the cytoskeleton (VDAC-1, vinculin, annexin). These observations suggest degradation of cell structures between post-mortem times D5 and D21 and the release of constitutive proteins whose became extractable. The major constituents of cytoskeleton and particularly components of myofibrils were absent of the clusters 3. The most frequently reported effects of proteolysis involve components of the extensive system of lateral attachment of myofibrils within Z-line (e.g., titin, nebulin, desmin, vinculin, troponin T, alpha-actinin), and attachment of myofibrils to the plasma membrane and to the basal lamina (e.g., vinculin, dystrophin, talin, ankyrin, laminin). Degradation of these proteins during post-mortem muscle aging has been reported in different studies (for reviews see refs *2*, *31*, *32*). Using 2-D electrophoresis, different studies (*33*–*35*) showed previously that fragments of actin appeared during muscle aging. In this study, we identified at D0 a fragment of actin in soluble fraction that, due to time of sampling (10 min post-mortem), could difficultly be related to post-mortem aging. None of the proteins presented above were found in the clusters, especially within the third cluster which was mainly constituted by protein fragments. One possible explanation is that some of these proteins have high molecular weights; thereby their proteolytic fragments would also be possibly large and thus could not be present in the gels. However, because the proteins of the three clusters we have chosen to identify did not constitute an exhaustive listing of all the possible proteome change during aging, it is possible that fragments of myofibrillar proteins or fragments of anchoring proteins were present on the gels and differential between post-mortem aging but not included in the clusters and consequently not identified.

Effect of Toughness (Te vs To) on Protein Abundance. Table 4 shows the number of spots whose quantity differs between Te and To groups. The proportion of spots significantly different between groups was higher than the proportion expected by chance (5%) in the insoluble fraction at D0 and D5. In other conditions, the proportion of spots influenced by group was insufficient. Spots significantly different between groups in the insoluble fraction at D0 and D5 were identified using peptide mass fingerprinting (**Tables 5** and **6**). At D0, 20 proteins were influenced by group (**Table 5**). We identified six proteins of the inner and outer membrane of mitochondria (prohibitin, mitofilin, elongation factor Tu, two voltage-dependent anion-selective channel protein1 and protein 2 and NADH-ubiquinone oxidoreductase) more abundant in Te group. Five other spots more abundant in the Te group were also identified: a 31 kDa fragment of actin, kelch-related protein 1, serum albumin, pyruvate kinase and adenylate kinase. The kelch-related protein 1 is abundant in muscle. Subcellular fractionation performed by Greenberg (*36*) showed its presence in both fractions (soluble and insoluble). Its function has not been reported, but binding localization with actin suggests that the protein plays a role in dynamic spatial organization of actin filaments.

Table 2. Bovine Longissimus Muscle Proteins Evidenced in Cluster 2 (See **Figure** 1) According to HCA Analysis

						M_w (kDa)/p*I*		mean value		
spot no.[a]	protein ID[b]	accession no.[b]	mowse score[c]	sequence coverage[d]	MP[e]	theor[f]	obsd[f]	at D0[g]	at D5[g]	at D21[g]
S2104	heat-shock protein beta-1 (HSP 27)	HSPB1_BOVIN	61	28	5	22.3/5.98	21.5/5.84	657	1462	1831
S4102	protein DJ-1	PARK7_HUMAN	72	43	10	19.8/6.33	21.5/6.05	2439	3811	4064
S2601	dihydropyrimidinase-related protein 2 (DRP-2)	DPYL2_BOVIN	82	28	11	62.2/5.95	60.2/5.62	–	230	321
S5005	histidine triad nucleotide-binding protein 1 (protein kinase C inhibitor 1)	HINT1_BOVIN	64	58	4	13.6/6.31	15/6.17	3355	5332	5783
S6103	adenylate kinase isoenzyme 1	KAD1_BOVIN	73	41	7	21.6/8.4	21/6.29	417	3483	4908
S5310	glycerol-3-phosphate dehydrogenase **Fgm**[h]	GPDA_MOUSE	77	30	11	37.4/6.83	31.7/6.21	763	1215	1494
S7601	phosphoglucomutase-1	PGM1_MOUSE	103	31	15	61.3/6.32	63.1/6.39	1211	3983	4913
S8002	ubiquitin	P62990|UBIQ_BOVIN	56	57	5	8.5/6.56	8.5/6.56	688	6999	9847
M5204	creatine kinase **Fgm**	KCRM_BOVIN	149	44	18	42.9/6.63	32.4/6.58	–	180	336
M4311	creatine kinase	KCRM_BOVIN	82	32	12	42.9/6.63	42.4/6.24	–	438	315
M5305	creatine kinase	KCRM_BOVIN	126	41	16	42.9/6.63	42.3/6.61	214	7236	6900
M5307	creatine kinase	KCRM_BOVIN	72	22	7	42.9/6.63	42/6.72	946	22802	20229
M5302	creatine kinase	KCRM_BOVIN	135	45	17	42.9/6.63	42.5/6.44	133	2909	2271
M6201	creatine kinase **Fgm**	KCRM_BOVIN	130	38	16	42.9/6.63	32.3/6.73	413	2815	4207
M4004	alpha crystallin B chain	CRYAB_BOVIN	133	61	13	20/6.76	20.6/6.23	–	1251	980
M6001	alpha crystallin B chain	CRYAB_BOVIN	87	45	10	20/6.76	20.4/6.77	616	7784	7635
M6014	myoglobin	MYG_BOVIN	132	73	12	16.9/6.97	17/6.9	105	858	697
M0108	14-3-3 protein gamma	1433G_BOVIN	102	36	9	28.1/4.8	29.9/4.76	57	616	702
M4106	heat-shock protein beta-1 (HSP 27)	HSPB1_BOVIN	99	61	10	22.3/5.98	22.3/5.98	–	63	68
M2102	heat-shock protein beta-1 (HSP 27)	HSPB1_BOVIN	85	53	9	22.3/5.98	22.3/5.43	–	258	105
M3103	heat-shock protein beta-1 (HSP 27)	HSPB1_BOVIN	85	53	9	22.3/5.98	22.3/5.74	–	145	83
M2106	heat-shock protein beta-1 (HSP 27)	HSPB1_BOVIN	103	69	10	22.3/5.98	22.3/5.62	121	3116	1937
M3104	heat-shock protein beta-1 (HSP 27)	HSPB1_BOVIN	117	76	11	22.3/5.98	22.3/5.83	247	1665	1577
M4609	WD repeat protein 1 (actin-interacting protein 1)	WDR1_MOUSE	71	15	12	66.2/6.12	66.2/6.24	6	165	92
M5608	AMP deaminase 1	AMPD1_HUMAN	88	19	17	86.4/6.43	85.6/6.7	10	104	86
M2110	actin, alpha **Fgm**	ACTS_BOVIN	74	22	7	42/5.23	30.1/5.55	–	33	80
M7211	glyceraldehyde-3-phosphate dehydrogenase	G3P_BOVIN	97	43	15	35.7/8.52	33.1/7.87	–	353	534
M0016	myosin regulatory light chain 2	MLRV_RAT	124	70	14	18.7/4.86	18.8/4.82	1693	7010	7210
M0107	14-3-3 protein epsilon	1433E_BOVIN	93	41	11	29.1/4.63	25.8/4.73	35	398	481
M3406	dihydrolipoamide succinyltransferase component of 2-oxoglutarate dehydrogenase complex	ODO2_PIG	64	15	7	48.9/9	51.9/5.82	–	40	48
M5402	pyruvate dehydrogenase E1 component alpha subunit	ODPA_MOUSE	136	43	20	43.2/8.49	45.8/6.52	–	46	59
M3004	heat shock protein beta-6	Q148F8| HSPB6_BOVIN	67	43	5	17.4/5.95	20.1/5.86	–	755	931
M1102	heat shock protein beta-1 (HSP 27)	Q3T149| HSPB1_BOVIN	80	36	6	22.3/5.98	22.5/5.32	8	301	181

[a] Spot number preceded by S corresponds to soluble fraction, and spot number preceded by M corresponds to insoluble fraction. [b] Protein name and accession numbers were derived from SWISS Prot database. [c] The MASCOT baseline significant score is 60. [d] % of coverage of the entire amino acid sequence. [e] Number of matched peptides in the database search. [f] MW and p*I*, theoretical (recorded in SWISS Prot database) and observed (calculated from the spot position on the gel). [g] Intensity mean value of tender and tough groups. (–) Spot intensity corresponds to intensity value lower than 15 ppm. [h] **Fgm**, protein fragment.

The remaining four identified spots were less abundant in the Te group: troponin C, full-length actin, glycogen phosphorylase and the four and a half LIM domains protein. This last protein, also known as cypher protein, is confined to the Z-line of skeletal muscle. Via its four and a half LIM domains, the protein combines with different proteins to regulate the function of cytoskeletal proteins and to connect cytoskeleton and contractile elements to the extracellular matrix. Cypher protein proteolysis has been correlated with the release of intact alpha-actinin from bovine myofibrils and would contribute to the weakening of the Z-line during meat aging (*37*, *34*). The protein was previously found overrepresented in the soluble fraction of tougher pig meat sampled 20 min after slaughter (*38*).

The most interesting feature found in the comparison of Te and To groups at D0 was the higher quantity of proteins constitutive of the mitochondrial membrane extracted in the insoluble fraction. It is well-known that the freeze–thaw cycle of muscle samples induces disruption of mitochondrial membrane integrity. This is commonly evidenced by the release of cytochrome *c* in the cytosolic fraction (*39*). Therefore, increased extractibility of mitochondrial membrane proteins would probably indicate a more extensive degradation of these membranes in the tender group which cannot, in the present study, be explained by a difference in freeze/thaw processes between samples. Moreover this degradation has occurred very early post-mortem and, thus, would not result from muscle aging. The simplest explanation would be an apoptotic process. Apoptosis is a major mode of programmed cell death used by multicellular organisms to eliminate dysfunctional cells. During apoptosis, mitochondria fragmentation happens early and participates to the activation of aspartate-specific, cysteine proteases (the caspase family), which cause the dismantlement of the cell (*40*). Caspase activation is a critical signal required to carry out apoptotic cell death (*41*). At slaughter, exsanguination deprives muscles suddenly of oxygen and micronutrients, these conditions leading muscle cells to engage in apoptotic processes (*42*). These authors reported evidence supporting the onset of apoptosis in post-mortem muscle: cell shrinkage, phosphatidylserine externalization and DNA fragmentation. In addition, the 31 kDa fragment of actin found overrepresented in the tender group may also support the apoptosis hypothesis because actin is known as a target of caspases and the fragment is used as an apoptosis marker (*41*). According to this hypothesis, the To group would not or at least would to a lesser extent engage in apoptotic processes, suggesting that regulating systems permitting attenuation of the apoptosis signal prevailed.

Table 3. Bovine Longissimus Muscle Proteins Evidenced in Cluster 3 (See **Figure** 1) According to HCA Analysis

						M_w (kDa)/p*I*		mean value		
spot no.[a]	protein ID[b]	accession no.[b]	mowse score[c]	sequence coverage[d]	MP[e]	theor[f]	obsd[f]	at D0[g]	at D5[g]	at D21[g]
S4108	phosphoglycerate kinase 1 **Fgm**[h]	PGK1_HORSE	122	39	15	44.4/8.64	22.3/6.1	–	–	8159
S4208	phosphoglycerate kinase 1 **Fgm**	PGK1_BOVIN	77	33	11	44.3/8.48	24.2/6.05	–	–	918
S7203	annexin A6 **Fgm**	ANXA6_BOVIN	68	23	14	69.7/5.43	30/6.43	–	–	1482
S2813	vinculin **Fgm**	VINC_PIG	79	8	10	123.7/5.63	82.1/5.61	–	–	177
S5411	heat shock cognate 71 kDa **Fgm**	HSP7C_CRIGR	62	14	7	70.7/5.24	38.6/6.23	–	33	419
S3717	heat shock 70 kDa protein 1A	Q27975|HS71A_BOVIN	107	30	15	70.2/5.68	69.4/5.99	519	696	1853
M7209	voltage-dependent anion-selective channel protein 1 (VDAC-1)	VDAC1_BOVIN	129	59	13	30.5/8.63	33/7.69	–	–	790
M5006	glyceraldehyde-3-phosphate dehydrogenase **Fgm**	G3P_SHEEP	63	25	7	34.7/7.83	21.7/6.61	–	–	75
M7118	glyceraldehyde-3-phosphate dehydrogenase **Fgm**	G3P_BOVIN	83	38	13	35.7/8.52	25.2/7.76	–	–	312
M7224	glyceraldehyde-3-phosphate dehydrogenase	G3P_BOVIN	96	43	14	35.7/8.52	33/7.34	–	–	948
M8135	glyceraldehyde-3-phosphate dehydrogenase **Fgm**	G3P_BOVIN	66	28	9	35.7/8.52	22.3/9	–	–	2101
M7009	glyceraldehyde-3-phosphate dehydrogenase **Fgm**	G3P_BOVIN	59	21	6	35.7/8.52	15.6/7.59	–	–	749
M8026	glyceraldehyde-3-phosphate dehydrogenase **Fgm**	G3P_BOVIN	74	23	9	35.7/8.52	16.5/8.5	–	–	464
M4109	beta-enolase **Fgm**	ENOB_RABIT	75	21	11	46.9/7.75	30.6/6.18	–	–	93
M5212	beta-enolase **Fgm**	ENOB_MOUSE	61	12	8	46.8/6.81	31.6/6.28	–	–	59
M4303	beta-enolase **Fgm**	ENOB_MOUSE	61	18	9	46.8/6.81	34.6/5.89	–	–	56
M4010	creatine kinase M-type **Fgm**	KCRM_BOVIN	61	17	7	42.9/6.63	16.4/6.2	–	–	30
M6108	creatine kinase M-type **Fgm**	KCRM_BOVIN	106	35	15	42.9/6.63	22.2/6.78	–	10	282
M2003	heat-shock protein beta-1 (HSP 27)	HSPB1_BOVIN	76	45	8	22.3/5.98	21.7/5.59	–	–	44
M3312	actin, alpha	ACTS_BOVIN	99	35	14	42/5.23	39.7/5.75	35	42	69

[a] Spot number preceded by S corresponds to soluble fraction, and spot number preceded by M corresponds to insoluble fraction. [b] Protein name and accession numbers were derived from SWISS Prot database. [c] The MASCOT baseline significant score is 60. [d] % of coverage of the entire amino acid sequence. [e] Number of matched peptides in the database search. [f] MW and p*I*, theoretical (recorded in SWISS Prot database) and observed (calculated from the spot position on the gel). [g] Intensity mean value of tender and tough groups. (–) Spot intensity corresponds to intensity value lower than 15 ppm. [h] **Fgm**, protein fragment.

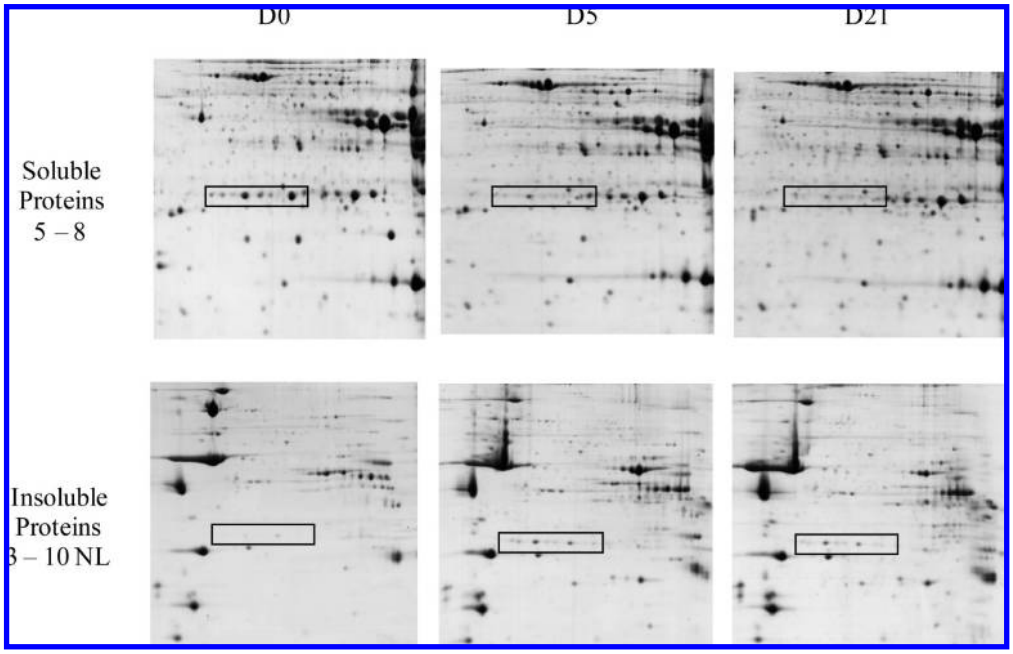

Figure 2. Representative 2-DE gel maps of soluble and insoluble fractions at the three post-mortem times. The gel sections encircled by rectangles correspond to HSP27 electrophoretic variants. The intensity of HSP 27 spots was high at D0 in the soluble fraction and decreased at D5 and D21. The intensity of HSP 27 spots was low at D0 in the insoluble fraction and increased at D5 and D21.

At D5, among the 15 proteins of insoluble fraction influenced by group, 11 were most abundant in the Te group (**Table 6**). The identified proteins more abundant in the Te group were fragments of glycolytic enzymes (CK and GAPDH), a spot of HSP 27 and three spots of troponin (T and I, fast-twitch isoforms). Increased quantity of fragments of glycolytic enzymes in the insoluble fraction was previously evidenced in clusters 2 and 3 characterizing meat aging. We thus suggest that the chemical process of muscle aging was more efficient in Te muscles. However, spots were different from those previously identified in clusters 2 and 3 (except spot M5204 corresponding to a fragment of CK). It is therefore possible that physical and chemical parameters governing protein insolubilization and proteolysis during aging were different in the Te group.

In cluster analysis, troponins were not found to be affected by aging. However, troponin T (Tn T) has been described in previous studies as a proteolysis substrate for μ-calpain under post-mortem conditions (*43*, *44*). Using 2-DE, Morzel (*34*) also showed that during pig muscle aging the quantity of full-length Tn T decreased and conversely Tn T fragments increased. Tn T

degradation is known to give a 30 kDa degradation product (*45*) whose quantity increased during muscle aging and was found related to meat tenderness (*46*). This fragment might correspond to the spot M7102 whose MW was estimated at 30 kDa. The spot intensity was higher in the Te group at D5 and remained stable at D21 (**Table 5**). In the To group the spot intensity increased between D5 and D21, suggesting that proteolysis was delayed. Bouley (*47*) showed 17 different electrophoretic variants of the Tn T, eleven belonging to fast muscle type. One spot of a full-length Tn T(f) (spot M8220) was found more intense in the Te group at D5. This difference may be due to higher extractibility of this isoform that could be explained by its release from a part of the myofibril network which is not extracted in the insoluble fraction

Table 4. Number of Spots Differing between Tender and Tough Groups Determined by ANOVA

	spots different between groups		
total no. of spots of the gels	at D0	at D5	at D21
soluble: 321	5	7	7
insoluble: 239	20 (15)[a]	15 (9)[a]	7

[a] Number in parentheses corresponds to the number of MS identified spots.

Table 5. Proteins Differentially Expressed between Tender and Tough Groups at D0

						M_w (kDa)/p*I*		intensity mean value		
spot no.[a]	protein ID[b]	accession no.[b]	mowse score[c]	sequence coverage[d]	MP[e]	theor[f]	obsd[f]	tender/ tough group D0 [g]	tender/t ough group D5 [g]	tender/ tough group D21 [g]
M0005	troponin C	TNNC2_RABIT	62	43	6	17.9/4.06	19.6/4	1016 /2225**	1525 /1581	3019 /2522
M1105	actin, alpha skeletal muscle **Fgm**[h]	ACTS_BOVIN	66	20	6	42/5.23	31.2/4.93	29.0/1.5**	19.6/28.8	19.2/25
M1606	Kelch-related protein 1 (sarcosin)	KBTBA_HUMAN	133	30	21	67.9/5.14	66.2/5.03	3493/2512*	2458/2037	1514/1304
M2105	prohibitin	PHB_BOVIN	76	43	9	29.7/5.57	29.7/5.57	31.8/6.9*	45.2/87.6	22.7/37.1
M2208	four and a half LIM domains protein	Q3ZBI6| FHL3_BOVIN	73	30	8	31.1/5.67	33.8/5.64	8.1/143*	102.5/123	99.5/47.9
M3309	actin, alpha skeletal muscle	ACTS_BOVIN	74	32	10	42/5.23	40.1/5.83	54.0/63.8*	75.5/56.7	113.1/121.6
M3602	serum albumin precursor	ALBU_BOVIN	69	25	12	69.2/5.82	65.7/5.71	142.4/35.7*	163.5/162.6	180.4/232.4
M3607	mitochondrial inner membrane protein (mitofilin)	IMMT_HUMAN	84	13	10	83.6/6.08	88.7/5.86	50.3/25.4*	53.7/63.4	49.8/42.9
M4414	elongation factor Tu, mitochondrial precursor	EFTU_BOVIN	103	34	13	49.3/6.72	45.5/6.12	30.6/12.4*	111.5/117	112.2/80.5
M5213	voltage-dependent anion-selective channel protein 2	VDAC2_BOVIN	93	28	8	31.6/7.48	31.6/6.5	56.2/19.1*	53.1/68.1	50/41
M5713	glycogen phosphorylase	PYGM_BOVIN	108	22	18	97.1/6.65	97.2/6.66	99.2/293.1*	752/524	1111/948
M6416	NADH-ubiquinone oxidoreductase 51 kDa subunit	NDUV1_BOVIN	148	42	18	50.6/8.37	52.1/6.83	42.7/11.78*	39.4/72.9	68.4/37.1
M6508	pyruvate kinase isozymeM1	KPYM_FELCA	114	30	19	57.8/7.23	60/7.03	59.3/20*	109.6/160.1	131.8/89.5
M7115	adenylate kinase isoenzyme 1	KAD1_BOVIN	119	64	13	21.6/8.4	22/7.57	296.6 /165.5*	916.1/1181	251.7/192.4
M7219	voltage-dependent anion-selective channel protein 1	VDAC1_BOVIN	129	59	13	30.5/8.63	31.4/7.62	99.7/19.2*	132.3/93.8	95.7/90

[a] Spot number preceded by M corresponds to insoluble fraction. Underlined spot number corresponds to a significant effect of time on spot intensity ($P < 0.05$). [b] Protein name and accession numbers were derived from SWISS Prot database. [c] The MASCOT baseline significant score is 60. [d] % of coverage of the entire amino acid sequence. [e] Number of matched peptides in the database search. [f] MW and p*I*, theoretical (recorded in SWISS Prot database) and observed (calculated from the spot position on the gel). [g] *$P < 0.05$, **$P < 0.01$, difference according to the Bonferroni pairewise comparison between groups. [h] **Fgm**, protein fragment.

Table 6. Proteins differentially expressed between Tender and Tough groups at D5

						M_w (kDa)/p*I*		intensity mean value		
spot no.[a]	protein ID[b]	accession no.[b]	mowse score[c]	sequence coverage[d]	MP[e]	theor[f]	obsd[f]	tender/ tough group D0 [g]	tender/ tough group D5 [g]	tender/ tough group D21 [g]
M4102	heat-shock protein beta-1 (HSP 27)	HSPB1_BOVIN	117	76	11	22.3/5.98	22/5.98	1.2/1.5	53.2/1.4**	362.4/227.4
M4105	creatine kinase **Fgm**[h]	KCRM_BOVIN	76	29	11	42.9/6.63	21.9/6.14	1.2/1.4	51.0/1.4*	317.1/295.1
M4418	glycogen phosphorylase, **Fgm**	PYGM_BOVIN	115	22	18	97.1/6.65	53.9/6.05	67.7/76.6	37.7/82.3**	30.1/23.7
M5204	creatine kinase, **Fgm**	KCRM_BOVIN	149	44	18	42.9/6.63	32.4/6.58	1.2/1.5	238.8 /121.4*	338.8/377.7
M6305	glyceraldehyde-3-phosphate dehydrogenase	G3P_BOVIN	73	37	12	35.7/8.52	35.2/6.84	614.1/905.9	1221/ 2150*	1221 /1128.5
M7102	troponin T, fast skeletal muscle (TnTf)	TNNT3_RABIT	60	25	10	32.8/5.63	30.4/7.39	1.2/1.5	314.8/ 1.42*	325.2/724.3
M8027	troponin I, fast skeletal muscle	TNNI2_RABIT	60	27	10	21/8.86	21/8.86	46.3/1.5	7632/3103*	22141/21906
M8122	glyceraldehyde-3-phosphate dehydrogenase **Fgm**	G3P_BOVIN	85	35	14	35.7/8.52	22.5/8.53	1.2/1.5	134.8/1.4*	3335.7/3435
M8129	glyceraldehyde-3-phosphate dehydrogenase **Fgm**	G3P_BOVIN	76	26	9	35.7/8.52	22.3/8.7	1.2/1.5	196.7/1.4*	3795/4034.7
M8220	troponin T, fast skeletal muscle (TnTf)	TNNT3_RABIT	67	26	11	32.8/5.63	32.2/8.72	1.2/1.5	863.4/0.6**	961.7/2168

[a] Spot number preceded by M corresponds to insoluble fraction. Underlined spot number corresponds to a significant effect of time on spot intensity ($P < 0.05$). [b] Protein name and accession numbers were derived from SWISS Prot database. [c] The MASCOT baseline significant score is 60. [d] % of coverage of the entire amino acid sequence. [e] Number of matched peptides in the database search. [f] MW and p*I*, theoretical (recorded in SWISS Prot database) and observed (calculated from the spot position on the gel). [g] *$P < 0.05$, **$P < 0.01$, difference according to the Bonferroni pairewise comparison between groups. [h] **Fgm**, protein fragment.

and remains in the final pellet. For technical reasons, the composition of this pellet was not analyzed, but it most probably contains cell insolubilized structures such as membrane debris, nuclei and certainly pieces of myofibril network. At D5 and D21 proteolysis may have accentuated dismantlement of these structures, releasing proteins which were solubilized. Just as the Tn T fragment (spot M7102), the post-mortem kinetic of the full-length Tn T(f) (spot M8220) was different between groups (**Table 5**). In the Te group the protein was released between D0 and D5 and remained stable at D21, while in the To group the protein was released between D5 and D21. In the same way, one spot of troponin I, more abundant in the Te group at D5 (spot M8027), had a comparable differential kinetics of release from the myofibril network (**Table 5**). The spot was not intense at D0 in both groups. Extractability of the protein increased twice in the Te group at D5 and increased again to reach the same intensity in both groups at D21. These results suggested that the kinetics of aging was different between groups. During aging the process of release and proteolysis of components of the myofibril network was accelerated in the Te group. Because the post-mortem aging rate was different between groups, post-mortem modifications of proteins whose intensity was different between groups were not evidenced by the cluster analysis.

Conclusion. This proteomic analysis showed that during muscle aging between D0 to D21 the solubility of some cytoplasmic proteins (HSPs and glycolytic enzymes) decreased, some proteins were fragmented (glycolytic enzymes, structural proteins) and some full length proteins were released from cellular structures like membranes and myofibrillar network (actin, troponin). The two groups (Te and To) were based on meat shear force measured 21 days post-mortem, but differences between Te and To proteomes were found within the first days of muscle aging (D0 and D5) suggesting precocity of implication of protein modifications in the determinism of mechanical properties of meat. Just after slaughter (at D0), the abundance of proteins of mitochondrial membrane and actin fragments in Te proteome suggested implication of apoptose process. To verify this hypothesis it would be interesting to test relationships between apoptose markers and meat shear force. At D5, the higher quantity of troponin found in the Te proteome suggested that the process of proteolysis and release of components of the myofibril network was accelerated in the Te group. We do not establish relationships between variations of meat shear force and the loss of solubility of cytoplasmic proteins. It may be explained by the fact that the ultimate pH of the two groups was not different. In order to verify a potential effect of protein insolubilization on beef meat tenderness as it is reported in pig meat, we should study relationships between the rate of pH fall in the first hours post-mortem and the rate of protein insolubilization.

ACKNOWLEDGMENT

The authors thank B. Meunier for advice in bioinformatics, members of the Herbivore Research Unit (INRA, Theix) for their technical assistance in this work, members of the experimental slaughterhouse and D. Krauss and members of the INRA Experimental Unit of Bourges for rearing and selecting the experimental animals.

LITERATURE CITED

(1) Jeremiah, L. E. Factors affecting consumption, selection and acceptability of meat purchases. *J. Consum. Stud. Home Economics* **1982**, *6*, 137–154.

(2) Koohmaraie, M. Biochemical factors regulating the toughening and tenderization processes of meat. *Meat Sci.* **1996**, *43*, S, S193−S201.

(3) Sentandreu, M. A.; Coulis, G.; Ouali, A. Role of muscle endopeptidases and their inhibitors in meat tenderness. *Trends Food Sci. Technol.* **2002**, *13*, 400–421.

(4) Monin, G. Ouali, A. Muscle differentiation and meat quality. In *Developments in Meat Science−5*; Ralston, L., Ed.; Elsevier Applied Science: London and New York, 1991; 253 pp.

(5) Boles, J. A.; Parrish, F. C.; Huiatt, T. W.; Robson, R. M. Effect of porcine stress syndrome on the solubility and degradation of myofibrillar cytoskeletal proteins. *J. Anim. Sci.* **1992**, *70*, 454–464.

(6) Minelli, G.; Culioli, J.; Vignon, X.; Monin, G. Postmortem changes in the mechanical properties and ultrastructure of the *longissimus* of two porcine breeds. *J. Muscle Foods* **1995**, *6*, 313–326.

(7) Fernandez, X.; Forslid, A.; Tornberg, E. The effect of high post-mortem temperature on the develoment of pale, soft and exudative pork: Interaction with ultimate pH. *Meat Sci.* **1994**, *37*, 133–147.

(8) Monin, G.; Larzul, C.; Le Roy, P.; Culioli, J.; Mourot, J.; Rousset-Akrim, S.; Talmant, A.; Touraille, C.; Sellier, P. Effect of the halothane genotype and slaughter weight on texture of pork. *J. Anim. Sci.* **1999**, *77*, 408–415.

(9) Dransfield, E. Optimisation of tenderisation, ageing and tenderness. *Meat Sci.* **1994**, *36*, 105–121.

(10) Hwang, I. H.; Thompson, J. M. The interaction between pH and temperature decline early post-mortem on the calpain system and objective tenderness in electrically stimulated beef *longissimus dorsi* muscle. *Meat Sci.* **2001**, *58*, 167–174.

(11) Rees, M. P.; Trout, G. R.; Warner, R. D. Tenderness of pork *m. longissimus thoracis et lumborum* after accelerated boning. Part I. Effect of temperature conditioning. *Meat Sci.* **2003**, *61*, 205–214.

(12) Hwang, I. H.; Park, B. Y.; Kim, J. H.; Cho, S. H.; Lee, J. M. Assessment of post-mortem proteolysis by gel-based analysis and its relationship to meat quality traits in pig *longissimus*. *Meat Sci.* **2005**, *69*, 79–91.

(13) Claeys, E.; De Smet, S.; Demeyer, D.; Geers, R.; Buys, N. Effect of rate of pH decline on muscle enzyme activities in two pig lines. *Meat Sci.* **2001**, *57*, 257–263.

(14) Gil, M.; Hortós, M.; Sárraga, C. Calpain and cathepsin activities, and protein extractability during ageing of *longissimus* porcine muscle from normal and PSE meat. *Food Chem.* **1998**, *63*, 385–390.

(15) Laville, E.; Sayd, T.; Terlouw, C.; Blinet, S.; Pinguet, J.; Fillaut, M.; Glénisson, J.; Chérel, P. Differences in pig muscle proteome according to HAL genotype: implications for meat quality defects. *J. Agric. Food Chem.* **2009**, *57*, 4913–4923.

(16) Pulford, D. J.; Fraga Vasquez, S.; Frost, D. F.; Fraser-Smith, E.; Dobbie, P.; Rosenvold, K. The intracellular distribution of small heat shock proteins in post-mortem beef is determined by ultimate pH. *Meat Sci.* **2008**, *79*, 623–630.

(17) Bernard, C.; Cassar-Malek, I.; Le Cunff, M.; Dubroeucq, H.; Renand, G.; Hocquette, J. F. New indicators of beef sensory quality revealed by expression of specific genes. *J. Agric. Food Chem.* **2007**, *55*, 5229–5237.

(18) Honikel, K. Reference methods for the assessment of physical characteristics of meat. *Meat Sci.* **1998**, *49*, 447–457.

(19) Hamelin, M.; Sayd, T.; Chambon, C.; Bouix, J.; Bibé, B.; Milenkovic, D.; Leveziel, H.; Georges, M.; Clop, A.; Marinova, P.; Laville, E. Proteomic analysis of the ovine "Belgian Texel" breed muscle hypertrophy. *J. Anim. Sci.* **2006**, *84*, 3266–3276.

(20) Morzel, M.; Chambon, C.; Lefèvre, F.; Paboeuf, G.; Laville, E. Modification of trout (Oncorhynchus mykiss) by preslaughter activity. *J. Agric. Food Chem.* **2006**, *54*, 2997–3001.

(21) Meunier, B.; Bouley, J.; Piec, I.; Bernard, C.; Picard, B.; Hocquette, J. F. Data analysis methods for detection of differential protein expression in two-dimensional gel electrophoresis. *Anal. Biochem.* **2005**, *340*, 226–230.

(22) Caraux, G.; Pinloche, S.; PermutMatrix, A graphical environment to arrange gene expression profiles in optimal linear order. *Bioinformatics* **2005**, *21*, 1280–1281.

(23) Meunier, B.; Dumas, E.; Piec, I.; Béchet, D.; Hébraud, M.; Hocquette, J. F. Assessment of hierachical clustering methodologies for proteomic data mining. *J. Proteome Res.* **2007**, *6*, 358–366.

(24) Miller, M.; Carr, M.; Ramsey, C.; Crockett, K.; Hoover, L. Consumer thresholds for establishing the value of beef tenderness. *J. Anim. Sci.* **2001**, *79*, 3062–3068.
(25) Jia, X.; Hollung, C.; Therkildsen, M.; Hildrum, K. I.; Bendixen, E. Proteome analysis of early post-mortem changes in two bovine muscle types: M. longissimus dorsi and M. semitendinosis. *Proteomics* **2006**, *6*, 936–944.
(26) Reddy, S.; Jones, A. D.; Cross, C. E.; Wong, P. S.-Y; Van der Vlet, A. Inactivation of creatine kinase by S-glutathionylation of the active-site cystein residue. *Biochem. J.* **2000**, *347*, 821–827.
(27) Cotgreave, I. A.; gerdes, R.; Shuppe-Koistinen, I.; Lind, C. S-glutathionylation of glyceraldehyde-3-phosphate dehydrogenase: role of thiol oxidation and catalysis by glutaredoxin. *Methods Enzymol.* **2002**, *348*, 175–182.
(28) Leichter, L. I.; Jakob, U. Protein thiol modifications visualized in vivo. *PLOS Biol.* **2004**, *2*, 1723–1737.
(29) Rogalla, T.; Ehrnsperger, M.; Preville, X.; Kotlyarov, A.; Lutsch, G.; Ducasse, C.; Paul, C.; Wieske, M.; Arrigo, A.-P.; Buchner, J.; Gaestel, M. Regulation of Hsp27 Oligomerization, Chaperone Function, and Protective Activity against Oxidative Stress/Tumor Necrosis Factor α by Phosphorylation. *J. Biol. Chem.* **1999**, *274*, 18947–18956.
(30) Bitar, K. N. HSP27 phosphorylation and interaction with actin-myosin in smooth muscle contraction. *Am. J. Physiol.* **2002**, *282*, G894–G903.
(31) Ouali, A. Meat tenderization: possible cause and mechanisms. A review. *J. Muscle Foods* **1990**, *1*, 129–165.
(32) Taylor, R. G.; Geesink, G. H.; Thompson, V. F.; Koohmaraie, M.; Goll, D. E. Is Z-disk degradation responsible for postmortem tenderization? *J. Anim. Sci.* **1995**, *73*, 1351–1367.
(33) Lametsch, R.; Roepstorff, P.; Bendixen, E. Identification of protein degradation during post-mortem storage of pig meat. *J. Agric. Food Chem.* **2002**, *50*, 5508–5512.
(34) Morzel, M.; Chambon, C.; Hamelin, M.; Santé-Lhoutellier, V.; Sayd, T.; Monin, G. proteome changes during pork meat ageing following use of two different pre-slaughter handling procedures. *Meat Sci.* **2004**, 689–696.
(35) Morzel, M.; Terlouw, C.; Chambon, C.; Micol, D.; Picard, B. Muscle proteome and meat eating qualities of Longissimus thoracis of "Blonde d'Aquitaine" young bulls: a central role of HSP27 isoforms. *Meat Sci.* **2008**, *78*, 297–304.
(36) Greenberg, C. C.; Connelly, P. S.; Daniels, M. P.; Horowits, R. Krp1 (Sarcosin) promotes lateral fusion of myofibril assembly intermediates in cultured mouse cardiomyocytes. *Exp. Cell Res.* **2008**, *314*, 1177–1191.
(37) Zhou, Q.; Ruiz-Lozano, P.; Martone, M. E.; Chen, J. Cypher, a striated muscle-restricted PDZ and LIM domain-containing protein binds to alpha-actinin 2 anD protein kinase C. *J. Biol. Chem.* **1999**, *247*, 19807–19813.
(38) Laville, E.; Sayd, T.; Terlouw, C.; Chambon, C.; Damon, M.; Larzul, C.; Le Roy, P.; Glénisson, J.; Chérel, P. Comparison of sarcoplasmic proteomes between two groups of pig muscles selected for shear force of cooked meat. *J. Agric. Food Chem.* **2007**, *55*, 5834–5841.
(39) Barbagli, C.; Serlupi Crescenzi, G. Influence of Freezing and Thawing on the Release of Cytochrome Oxidase from Chicken's Liver and from Beef and Trout Muscle. *J. Food Sci.* **2006**, *46*, 491–493.
(40) Youle, R. J.; Karbowski, M. Mitochondrial fission in apoptosis. *Nat. Rev. Mol. Cell Biol.* **2005**, *6*, 657–663.
(41) Yang, F.; Sun, X.; Beech, W.; Teter, B.; Wu, S.; Sigel, J.; Vinters, H. V.; Frautschy, S. A.; Cole, G. M. Antibody to caspase-cleaved actin detects apoptosis in differentiated neuroblastoma and plaque-associated neurons and microglia in Alzheimer's disease. *Am. J. Pathol.* **1998**, *152*, 379–389.
(42) Herrera-Mendez, C. H.; Becila, S.; Boudjellalb, A.; Ouali, A. Meat ageing: Reconsideration of the current concept. *Trends Food Sci. Technol.* **2006**, *17*, 394–405.
(43) Huff-Lonergan, E.; Mitsuhashi, T.; Beekman, D. D.; Parrish, F. C. Jr; Olson, D. G.; Robson, R. M. Proteolysis of specific muscle structural proteins by mu-calpain at low pH and temperature is similar to degradation in postmortem bovine muscle. *J. Anim. Sci.* **1996**, *74*, 993–1008.
(44) Lametsch, R.; Roepstorff, P.; Moller, H. S.; Bendixen, E. Identification of myofibrillar substrates for μ-calpain. *Meat Sci.* **2004**, *68*, 515–521.
(45) Ho, C. Y.; Stromer, M. H.; Robson, R. M. Identification of the 30 kDa polypeptide in post-mortem skeletal muscle as a degradation product of Troponin T. *Biochimie* **1994**, *76*, 369–375.
(46) Tsitsilonis, O. E.; Stoeva, S.; Echner, H.; Balafas, A.; Margomenou, L.; Haralabos, L.; Katsoulas, H. L.; Troy, D. J.; Voelter, W.; Papamichail, M.; Lymberi, P. A skeletal muscle troponin T specific ELISA based on the use of an antibody against the soluble troponin T (16-31) fragment. *J. Immunol. Methods* **2002**, *268* (2), 141–148.
(47) Bouley, J.; Chambon, C.; Picard, B. Mapping of bovine skeletal muscle proteins using two-dimensional gel electrophoresis and mass spectrometry. *Proteomics* **2004**, *4*, 1811–1824.

Received for review June 8, 2009. Revised manuscript received September 24, 2009. Accepted October 6, 2009. This study was funded by a national grant from the Agence Nationale de la Recherche and from APIS-GENE (GENANIMAL call, national program AGENAE) for the project MUGENE (GENEs of the MUscle tissue).